

Article citation info:

Fang P, Sui X, Zhang A, Wang D, Yin L, Fusion model based RUL prediction method of lithium-ion battery under working conditions, *Eksploracja i Niezawodność – Maintenance and Reliability* 2024; 26(3) <http://doi.org/10.17531/ein/186537>

Fusion model based RUL prediction method of lithium-ion battery under working conditions

Indexed by:



Pengya Fang^{a,*}, Xiaoxiao Sui^b, Anhao Zhang^c, Di Wang^c, Liping Yin^a

^a School of Aero Engine, Zhengzhou University of Aeronautics, China

^b Chongqing Research Institute of Harbin Institute of Technology, China

^c School of Materials Science and Engineering, Zhengzhou University of Aeronautics, China

Highlights

- A novel approach for constructing the feature space of lithium-ion battery by fusing the traditional manual features and the features extracted with 1DCNN.
- A SVM-LSTM fusion model proposed for estimating the battery capacity through exploring the spatial and temporal relationship of features.
- A feasible and precise RUL prediction method suitable for the actual engineering background of unknown historical capacity data of battery.

Abstract

Under working conditions, since the remaining useful life (RUL) prediction of lithium-ion battery is subject to uncertainties of random charging and discharging, and infeasibility of battery capacity test, a fusion model based RUL prediction method was proposed. First, the feature learning method of lithium-ion batteries was developed by synthesizing manual extraction and one-dimensional convolutional neural network (1DCNN) extraction. Then, a fused method was proposed to estimate the historical available capacity through exploring the spatial and temporal relationship of features, and the long short-term memory (LSTM) network model was adopted for predicting the RUL of lithium-ion battery. The proposed method was verified through the comparison of different methods, and the results show that it can realize highly precise and stable capacity estimation and RUL prediction under working conditions.

Keywords

lithium-ion battery, available capacity estimation, remaining useful life (RUL), health feature extraction, data-driven approach.

This is an open access article under the CC BY license (<https://creativecommons.org/licenses/by/4.0/>)

1. Introduction

In recent years, the world is suffering from deteriorating ecological environment and serious resource consumption, so new energy vehicles will gradually become the new direction and hotspot field of zero-carbon economic development. As the best choice of power reserve for current electric vehicles, the service performance and operating reliability of lithium-ion battery is the key factor affecting the development of new energy industry. The users can get to know the health status of lithium-ion battery through RUL prediction, to provide important basis for preventative maintenance of battery.

There are two categories of mainstream methods for RUL prediction of lithium-ion battery: model-based approach and data-driven approach¹. Lithium-ion battery model is the key of model-based approach, and electrochemical model, equivalent circuit model and empirical model are the most commonly used ones. Electrochemical model is to analyze the degradation laws of the operating performance of battery in charging and discharging cycles based on the quantification of the micro change process of internal electrochemical reactions of lithium-ion battery. By reflecting the degradation laws of external state

(*) Corresponding author.

E-mail addresses:

P. Fang (ORCID: 0000000327931924) pyfang12@163.com, X. Sui (ORCID: 0000000201446667) suixxazj@163.com, A. Zhang (ORCID: 0000000274588316) relaxing1121@163.com, D. Wang (ORCID: 0009000676978963) wangdbm@163.com, L. Yin yinliping@zua.edu.cn

monitoring data through internal mechanism, it further predicts the RUL of lithium-ion battery³. Equivalent circuit model is mainly composed of the ideal voltage source, resistance, parallel coupled resistance-capacitance pairs and other simple circuit components. Characterized by the simulation of the dynamic features of battery, few model parameters and easy parameter identification, it is one of the commonly used models of battery management system (BMS)⁶. Empirical model is to construct the degradation model of battery by analyzing the decay laws of the health features of lithium-ion battery along with the time variation, identify and update the parameters of degradation model based on index model, multinomial model or filtering algorithm, and then predicts the RUL of lithium-ion battery based on extrapolation⁹. As for the model-based approach, the precision of RUL prediction largely relies on the accuracy and generalization of the battery model built, with certain limitations.

The data-driven prediction method is independent of the internal chemical reaction of lithium-ion battery. Based on black-box modeling method, it performs RUL prediction by direct exploration of the health features either from external monitoring data of battery such as current, voltage, charging and discharging time, and temperature, or the internal state parameters like impedance and capacity¹⁰. Commonly used prediction methods include autoregressive models (ARM), support vector machine (SVM), relevance vector machine (RVM), and artificial neural network (ANN). Specific to the nonlinear aggravated degradation of lithium-ion battery performance in later stage of service life, Long et al.¹³ introduced accelerated degradation correction factor and built a nonlinear ARM for RUL prediction. Wei et al.¹⁴ took the features extracted from the current data in constant voltage charging stage as the input variable and the charging capacity as the state variable based on the current data of lithium-ion battery in constant-voltage charging stage, to build the SVM state space for the available capacity prediction of battery. But the kernel function of SVM should meet Mercer conditions, and there is a problem of insufficient sparsity. For this purpose, Liu et al.¹⁵ proposed the method of on-line RUL prediction of lithium-ion battery based on the RVM algorithm with the highly sparse kernel function, which improved the prediction precision and output the uncertainty information of prediction results.

Along with the development of machine learning technology, shallow neural network and deep neural network based on deep learning are gradually applied in RUL prediction study of lithium-ion battery. Wu et al.¹⁶ selected the voltage values in charging stage as the health factor to build the indirect RUL prediction model of lithium-ion battery based on ANN. However, when the input data increase, ANN-based model may easily be trapped local optimization or overfitting in later stage. For effective matching of big data sample, Cao et al.¹⁷ extracted the features of lithium-ion battery data and performed integration through Autoencoder, and then used deep neural network for RUL prediction. Wang¹⁸ constructed the health indicator of lithium-ion battery using kernel principal component analysis (KPCA), built the indirect RUL prediction model by LSTM network, and carried out test verification. Li et al.¹⁹ constructed a 1DCNN with fewer network parameters taking the voltage, current, and temperature curves of lithium-ion battery in charging stage as the input, for successful prediction of battery capacity. Gao et al.²⁰ developed a RUL prediction model by fusing CNN and bi-directional long short-term memory (Bi-LSTM) network, which features higher prediction precision and good stability compared with single method. Recently, recurrent neural networks (RNNs) represented by LSTM have become one of the most popular methods in the study of RUL prediction, and some improved methods are gradually developed and applied²¹.

On the whole, the data-driven prediction method can perform model training based on the monitoring data of external battery features, for highly precise RUL prediction. It is a technological path much concerned at present. However, present studies are mostly centered on the improvement of algorithm precision and efficiency in simple application scenarios, in lack of deep study on the characteristics of battery in actual operating conditions. To this end, this paper sorted out two bottleneck issues of RUL prediction for the lithium-ion battery in operation. First, due to different driving habits of users, the discharge rate and depth, charging state, and aging state of lithium-ion battery exhibit randomness, and the charge-discharge curve show inconsistency in different cycles. In such scenario, how to effectively extract more representative and robust health features? Second, in actual working condition, the real-time available capacity of battery cannot be obtained since

a capacity test cannot be done on board just like the case in the laboratory environment, and complex service conditions lead to the nonlinear and discontinuous behavior of battery performance degradation, impeding the smooth progress of battery RUL prediction. How to perform RUL prediction based on external monitoring parameters such as current and voltage when the historical available capacity is unknown?

Aiming to the above two questions, this paper studied the RUL prediction methods of lithium-ion battery under working conditions. The remaining chapters of this paper are organized as follows. Chapter II performed cycle life test under constant

current-constant voltage (CC-CV) charge mode and New European Driving Cycle (NEDC) discharge mode, to acquire the current, voltage, and other external monitoring data of the battery in charging and discharging stage. Chapter III studied the methods of extracting health features of lithium-ion battery by manual knowledge and machine learning, to provide data basis for RUL prediction model. Chapter IV studied the method of estimating the available capacity of lithium-ion battery based on feature parameters, and then constructed the deep learning network for RUL prediction of lithium-ion battery. To enhance the readability, Figure 1 outlines the main work of this paper.

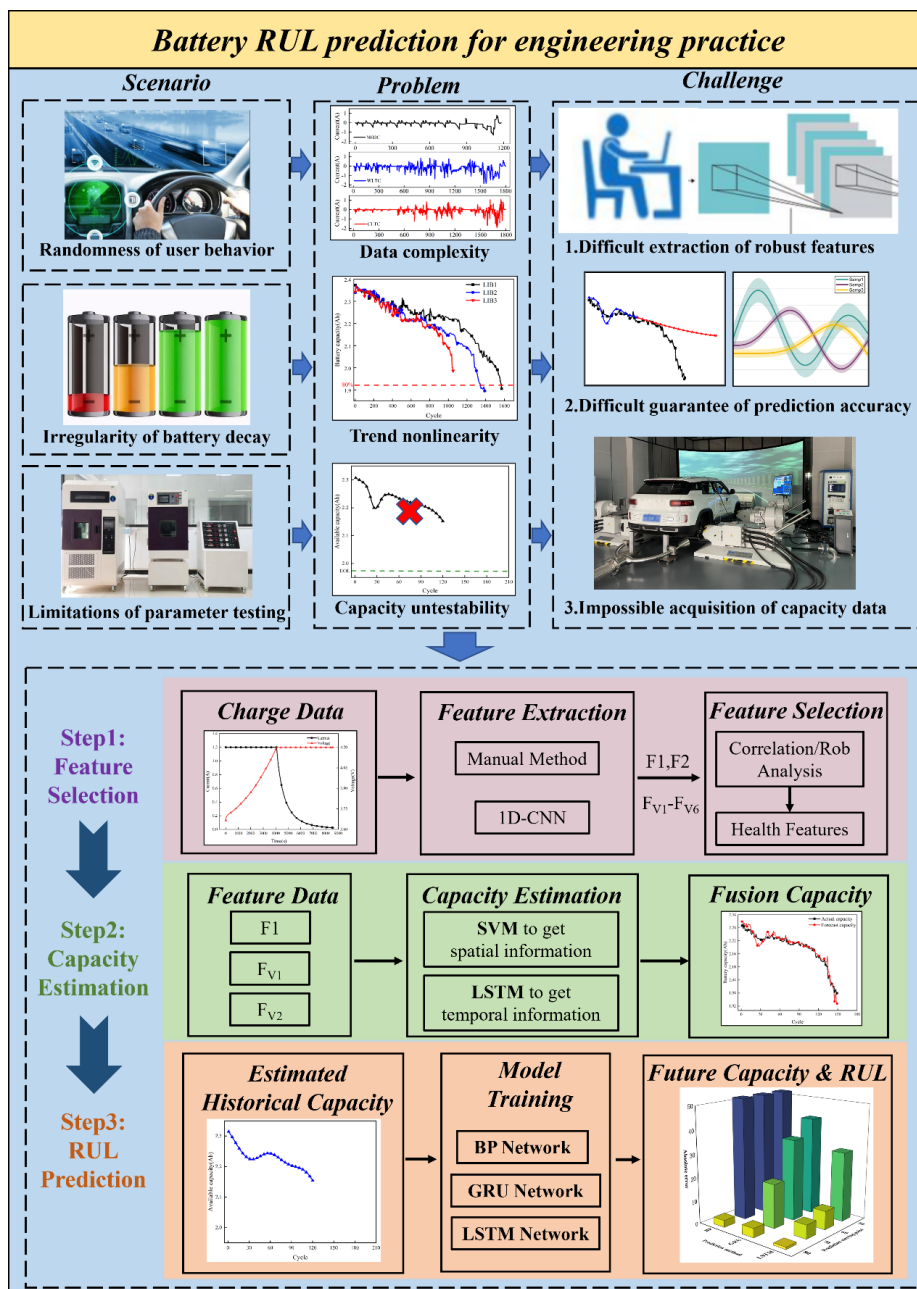


Figure 1. Table of content.

2. Cycle life test of lithium-ion battery

In the cycle life test of lithium-ion battery, the 18650 ternary lithium battery was selected as the research object. Set up the test platform as shown in Figure 2. The battery test system client

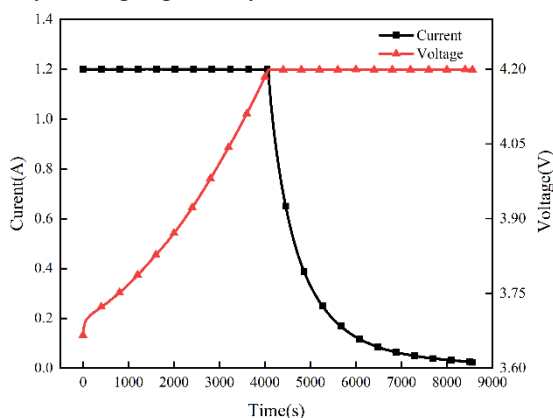
facilitates the configuration of experimental parameters and the collection of data, while the thermostatic chamber furnishes a controlled and stable test environment for Li-ion batteries. Furthermore, the cycle test equipment is employed to apply specific loads during the test procedures.



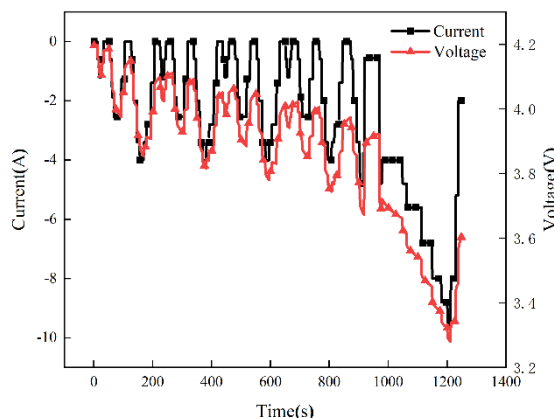
Figure 2. Lithium battery test platform.

For the cycle life test of the lithium-ion battery, the CC–CV charge mode and the NEDC discharge mode were adopted. The change trends of voltage and current in the charge stage are shown in Figure 3 (a), and the change curves of voltage and current in the discharge stage are shown in Figure 3 (b). As can be seen from Figure 3 (a), in the constant current charging stage, the battery voltage gradually increases till it reaches the

charging cut-off voltage of 4.2 V as the charging time increases; in the constant voltage charging stage, the battery current gradually decreases till it reaches the charging cut-off current of 24 mA as the charging time increases. It can be seen from the NEDC discharge condition in Figure 3 (b) that the variation trend of voltage and current fluctuates greatly and the stabilization time lasts for a short time.



(a) CC–CV charging voltage and current.



(b) NEDC discharging voltage and current.

Figure 3. Voltage and current curves in the charge-discharge stage of lithium-ion batteries.

Adopting the aforementioned charge-discharge mode, the cycle life tests of three groups of lithium-ion batteries (capacity 2.4 Ah) of LiB1, LiB2, and LIB3 were carried out. Figure 4 shows the degradation curve of the actual available capacity of three groups of lithium-ion batteries with the cycle number. Here, the horizontal axis represents the number of charge-discharge cycles, while in the subsequent sections, the term

“cycle” in figures refers to the number of capacity testing cycles.

After 1,570, 1,390, and 1,005 charge-discharge cycle tests of three groups of lithium-ion batteries, LiB1, LiB2, and LIB3, the actual available capacity decayed to 1.906 Ah, 1.896 Ah, and 1.98 Ah, and the corresponding SOH (calculated by available capacity) of the batteries were 79.4%, 79.0% and 82.5% respectively. Specially, due to certain fault, battery LIB3 is no

longer able to complete a full NEDC discharge cycle, indicating that the battery has reached the end of its lifespan. The actual available capacity of lithium-ion batteries decreased slowly in the initial stage of the charge-discharge cycle life test but decreased obviously in the later stage.

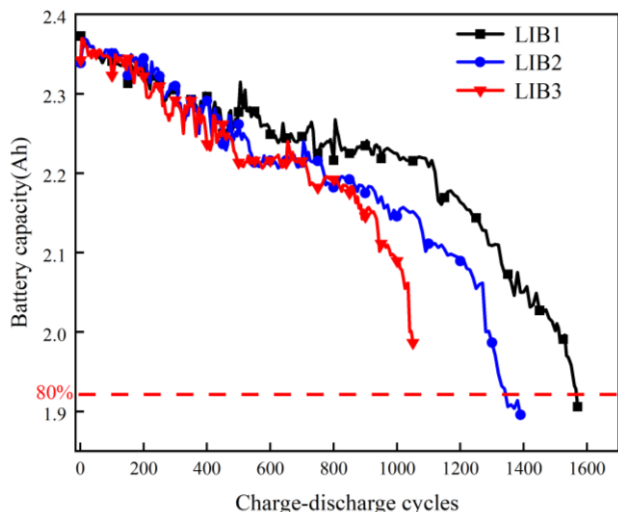


Figure 4. Capacity degradations versus cycle number for lithium-ion batteries.

3. Health feature extraction of lithium-ion battery under working conditions

The health features of lithium-ion battery are vital to the precision of battery capacity estimation and RUL prediction. Under working conditions, the battery features fixed charging strategy, and relatively stable charge mode, while the discharge mode is more complicated, with prominent phenomenon of random discharge. Therefore, only the voltage and current data in the charging stage were selected as input to study the method of extracting the health features of lithium-ion batteries. Although the traditional manual extraction method can extract some interpretable features according to experts' experience, it is subjective and insufficient to explore the deep characteristics of data. The charging data is only a part of the battery charge-discharge cycle data. To get the health status of the battery based on these data, it is necessary to explore deep into the charging data. Therefore, the health features of the charging data are extracted manually in this paper, and then the CNN method is introduced for supplementary feature extraction.

3.1 Health feature extraction of battery based on traditional methods

Under different cycle periods, the voltage curve of the battery

in constant current charging stage is shown in Figure 5, and the current curve in constant voltage charging stage is shown in Figure 6. For the constant current charging stage, the time for the battery voltage to rise from the initial voltage to the charging cut-off voltage is different. The more cycles of the battery are, the shorter the charging time will be, indicating a negative correlation between them. For the constant voltage charging stage, the time for the voltage to drop from the initial charging current to the cut-off current is also different. The more cycles of the battery are, the longer the charging time will be, indicating a positive correlation between them. Therefore, the charging time interval of the battery in the two stages of constant current charging and constant voltage charging is used as the manually extracted features.

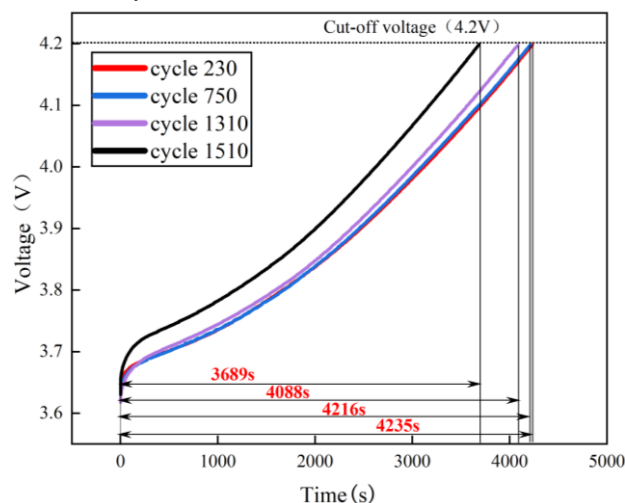


Figure 5. Voltage curves during the constant current charging stage under various aging conditions.

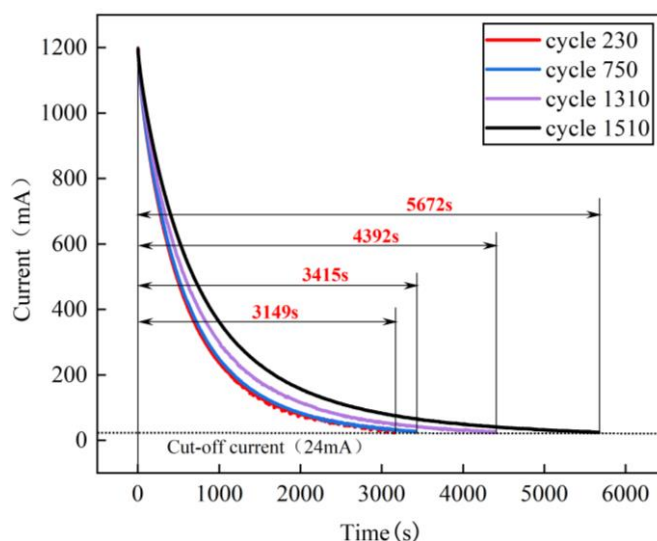


Figure 6. Current curves during the constant voltage charging stage under various aging conditions.

Considering the phenomenon that the battery is charged

before it is fully discharged and it has power cut off before it is fully charged under working conditions, a low voltage point, and a high voltage point are set in the middle of constant current charging, and the charging time interval between two fixed voltage points under different cycles is calculated as the first extracted health feature (recorded as F_1), which is called equal voltage rise charging interval. Similarly, in the constant voltage charging stage, a high current point and a low current point are set, and the charging time interval between two fixed current points under different cycles is calculated as the second extracted health feature (recorded as F_2), which is called equal current drop charging interval. Batteries LIB1 and LIB2 are selected for feature extraction, and the obtained health feature F_1 is shown in Figure 7 and health feature F_2 is shown in Figure 8.

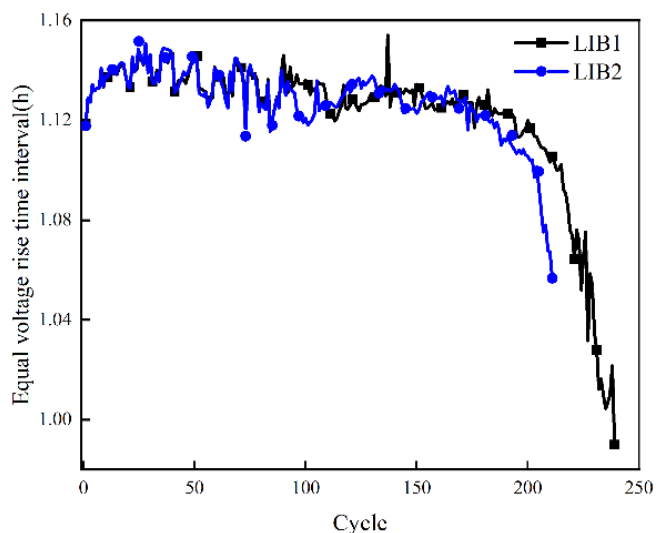


Figure 7. Change trend of health feature F_1 .

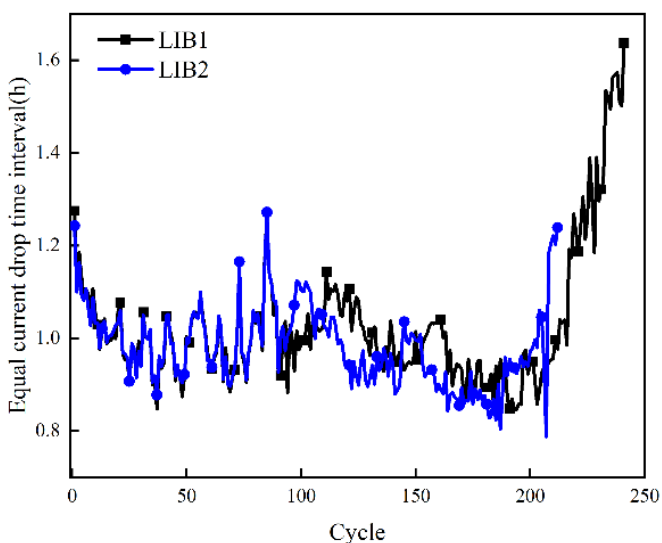


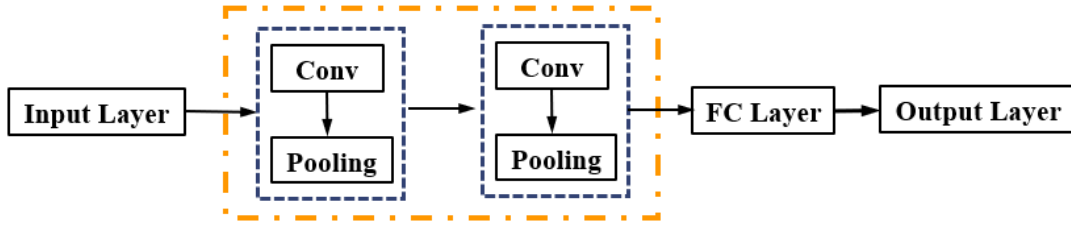
Figure 8. Change trend of health feature F_2 .

It can be seen that with the increase of cycle number for

lithium-ion batteries, the equal voltage rise charging interval F_1 generally shows a decreasing trend, and the equal current drop charging interval F_2 basically shows an increasing trend. Compared with F_2 , F_1 curve has less fluctuation and better stability. In addition, as the number of charge-discharge cycles increases, the active substances in the battery decrease, the SEI film gradually thickens and the side reactions appear, the decay of the available capacity of the battery speeds up, represented by the gradual acceleration of the change rate of health feature F_1 and F_2 . This rule is also consistent with the changing trend of battery capacity in Figure 1, which further verifies the rationality of F_1 and F_2 . However, it was also found that F_1 and F_2 changed obviously in the late period of battery performance degradation, but did not change significantly in the middle and early period.

3.2 Health feature extraction of battery based on CNN

Although the manually extracted features can reflect the health state of the battery, they only employ the interval information corresponding to the charging time in the two stages of constant current charging and constant voltage charging, neglecting a large number of rich and valuable temporal information contained by the data of voltage and current in the charging stage. Therefore, this section applies the 1DCNN method to perform convolution and pooling on the current and voltage temporal data of lithium-ion batteries, for automatic feature extraction of deep information of lithium-ion battery data sets. A 1DCNN network structure as shown in Figure 9 is constructed by taking the voltage value in constant-current charging stage (recorded as CCV) and the current value in constant-voltage charging stage (recorded as CVI) of lithium-ion battery as the input data sets and the available capacity of the battery as the output data set, respectively, and the output of the last pool layer is extracted as the health feature. There are three features extracted based on CCV data, which are denoted as F_{V1} , F_{V2} , F_{V3} ; there are also three features extracted based on CVI data extraction, which are denoted as F_{I1} , F_{I2} , F_{I3} . The hyperparameters of 1DCNN network are listed in Table 1, and the Dropout rate of the full connection layer is set to 1%. Adam optimizer is selected to minimize the total loss, which is expressed as the MSE function. The initial learning rate and decay rate are set to 0.009 and 0.005, respectively.



Convolutional + Pooling => Spatial features

Figure 9. 1DCNN network for health feature extraction.

Table 1. 1DCNN network hyperparameter settings.

| 1DCNN network layers | In channel | Out channel | Kernel size | Stride | Padding |
|----------------------|------------|-------------|-------------|--------|---------|
| Conv1 | 1 | 3 | 17 | 15 | 1 |
| Pooling1 | — | — | 3 | 2 | — |
| Conv2 | 3 | 3 | 10 | 8 | 1 |
| Pooling2 | — | — | 2 | 2 | — |

Select LIB1 data for network training and LIB2 data for network testing. Limited by space, only two features of F_{V1} , F_{V2} for LIB2 battery are listed here, as shown in Figures 10 and 11.

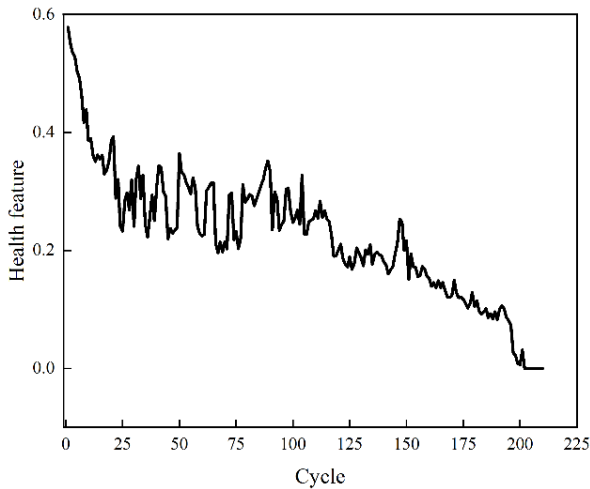


Figure 10. Change trend of health feature F_{V1} .

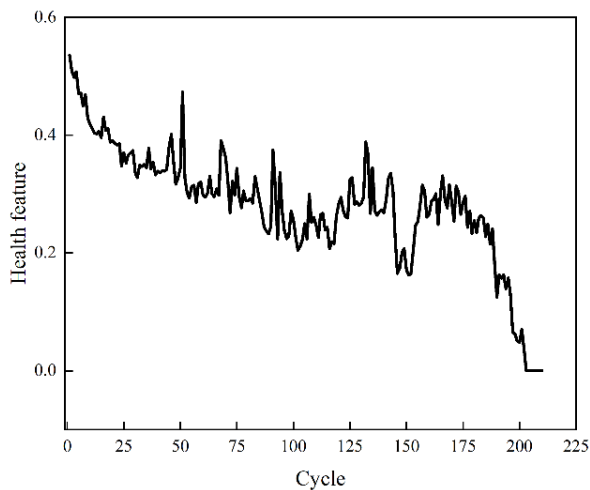


Figure 11. Change trend of health feature F_{V2} .

3.3 Health feature evaluation and screening

As what mentioned before, there are 2 features for manual extraction and 6 features for CNN extraction. Predicting the RUL by directly selecting those features may reduce the calculation efficiency and generalization of prediction model due to the irrelevant or redundant information contained in the health features. Therefore, in this paper, the health features extracted are evaluated according to two common evaluation criteria: correlation and robustness to give basis for feature screening. The correlation index R_{XY} and robustness index $Rob(F)$ can be calculated according to formulas (1) and (2).

$$R_{XY} = \frac{\sum(F_i - \bar{F})(Q_i - \bar{Q})}{\sqrt{\sum(F_i - \bar{F})^2} \sqrt{\sum(Q_i - \bar{Q})^2}} \quad (1)$$

Where:

F_i — Value of health feature for the i -th cycle;

Q_i — Value of available capacity for the i -th cycle;

\bar{F} — Mean of health feature;

\bar{Q} — Mean of available capacity.

$$Rob(F) = \frac{\sum_{i=1}^L \exp(-|R_L|)}{L} \quad (2)$$

Where:

F_L — Component of stable trend;

R_L — Component of random remainder, $R_L = F - F_L$;

L — Length of feature data.

According to the formulas above, the greater the absolute value of R_{XY} is, the stronger the correlation between the health features and actual available capacity will be; the greater the $Rob(F)$ value is, the stronger the robustness of health features will be.

Analyze battery LIB2 and include the calculated results of correlation and robustness of all health features in Table 2. It is shown that for manual extraction method, health feature F_1 exhibits strong correlation and robustness, while health feature F_2 exhibits higher robustness, but lower correlation. As for the 1DCNN method, both F_{V1} and F_{V2} exhibit higher correlation and stronger robustness, while F_{V3} exhibits higher robustness but lower correlation; F_{I1} , F_{I2} and F_{I3} exhibit higher robustness but relatively low correlation.

Table 2. Evaluation results of health features for battery LIB2.

| Methods | Health features | R_{XY} | $Rob(F)$ |
|-------------------|-----------------|----------|----------|
| Manual extraction | F1 | 0.815 | 0.998 |
| | F2 | 0.203 | 0.975 |
| 1DCNN | F_{V1} | 0.845 | 0.876 |
| | F_{V2} | 0.910 | 0.949 |
| | F_{V3} | 0.241 | 0.945 |
| | F_{I1} | 0.635 | 0.943 |
| | F_{I2} | 0.725 | 0.941 |
| | F_{I3} | 0.689 | 0.945 |

According to the evaluation results above-mentioned, three health features of F_1 , F_{V1} and F_{V2} are screened in this paper to build the health feature space, providing data basis for follow-up RUL prediction of lithium-ion batteries.

4. RUL prediction of lithium-ion battery in working conditions

Differing from battery test in labs, in actual working condition, a capacity test of battery cannot be carried out, and accordingly, the real-time available capacity of battery cannot be obtained. Therefore, the estimation method of battery available capacity based on the health features was studied, and then the RUL prediction of lithium-ion battery was explored.

4.1 Available capacity estimation for lithium-ion battery

In this section, the data of LIB2 battery was applied to train the battery capacity estimation model, and the available capacity of

LIB3 battery was estimated with the trained model. To better explore the mapping relationship between health features and available capacity, the SVM and LSTM model was employed to mine and capture the spatial and temporal relation among battery health features in different cycles, respectively. Then, a method synthesizing SVM and LSTM was developed. It is noted that since the shuffle method was applied to train the model, the validation samples were randomly selected. As a result, the following figures may exhibit slight variations in representing the estimation effect. Considering the incomplete activation behavior of batteries in the early stage of test, the front-end test data was cut off when evaluating and predicting the battery capacity.

(1) SVM model

In consideration of the nonlinear trend of battery capacity degradation, radial basis function is selected as the kernel function of SVM model for capacity estimation. The setting of penalty factor C affects the generalization ability of estimation model. The greater the value of penalty factor C is, the weaker the generalization ability of estimation model will be; the penalty factor C is determined as 10 after training. Figures 12 and 13 show the curves of capacity estimation versus cycle number for batteries LIB2 and LIB3.

It can be seen that the relative error for capacity estimation of lithium-ion battery LIB2 is basically small, and reaches 8.2% only at the ending stage of battery life. In consideration that the battery is in a poor health at the moment, the chemical reaction inside is unstable relatively, resulting in larger prediction error. Validating the estimation model with lithium-ion battery LIB3, the overall prediction error is basically better controlled and the error is relatively large at the end of battery life as well. It shows that in the most stages of battery life, SVM model established has higher precision for battery capacity estimation, and the precision declines to certain extent only at the end of the life. Moreover, the estimation precision is high relatively in different cycles, but the capacity estimation results fluctuate greatly in the entire test period. The reason lies in that for SVM model, only the spatial mapping relation between battery capacity and health features in certain cycle is taken into account, while the temporal relationship of health features in different cycles is failed to be fully considered, which has larger influence on the stability of estimation results.

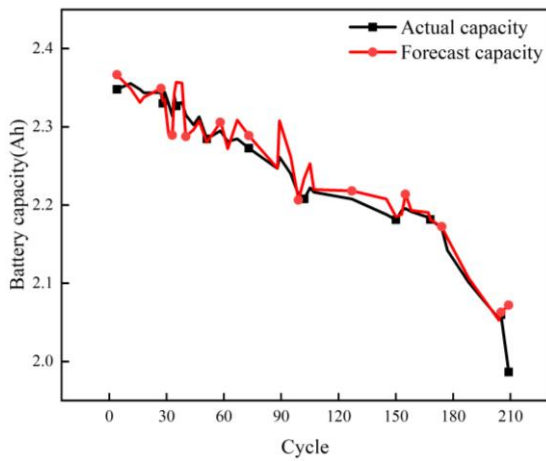


Figure 12. LIB2 capacity estimation results based on SVM.

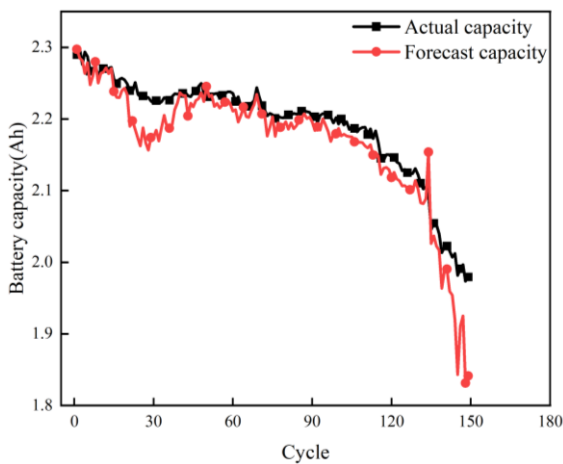


Figure 13. LIB3 capacity estimation results based on SVM.

(2) LSTM model

To make the best of the temporal information among health features of lithium-ion batteries in different cycles, the available capacity of lithium-ion batteries is estimated based on LSTM, and the curves of capacity estimation for batteries LIB2 and LIB3 are shown in Figures 14 and 15.

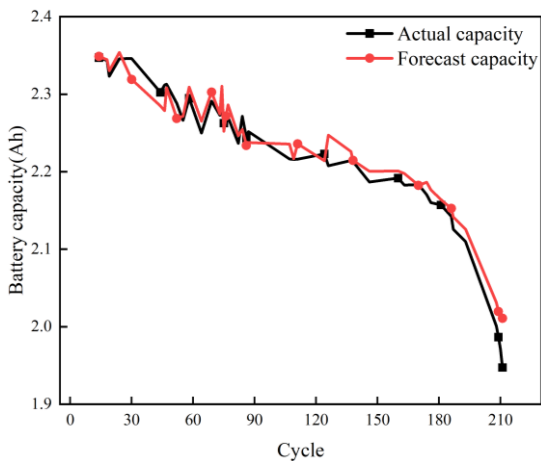


Figure 14. LIB2 capacity estimation results based on LSTM.

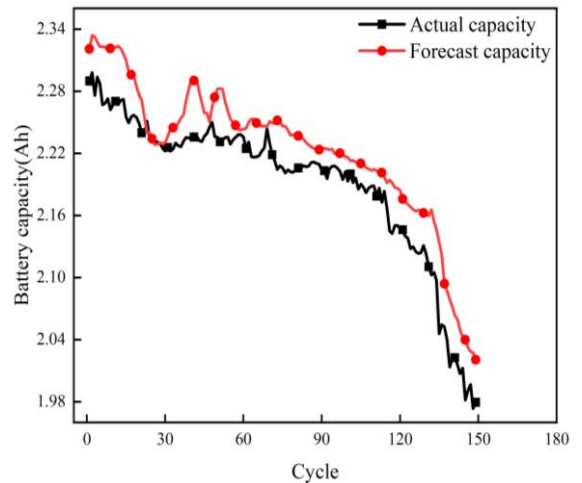


Figure 15. LIB3 capacity estimation results based on LSTM.

The maximum relative error for capacity estimation of lithium-ion battery LIB2 is lower than 4%, and that of lithium-ion battery LIB3 is lower than 5%. In comparison with SVM method, the maximum relative error of LSTM method reduces and the prediction curve is smoother. The reason lies in that during battery capacity estimation in certain cycle, only the health feature of battery in the cycle are input for SVM method, and in case of great difference and volatility for the health feature, the precision of model estimation is greatly affected. While for LSTM method, the temporal relationship among features in different cycles is put into full consideration, which can better seize the battery performance change trend, and therefore, reduces the volatility of capacity estimation results and improves the estimation precision and robustness at different moments.

(3) SVM-LSTM fusion model

To synthesize the advantages of two models SVM and LSTM, in this paper, it is explored to fuse the estimation results based on SVM and LSTM with weighted mean method. For simplifying the weight assignment problem, the estimation results are fused through arithmetic mean as below:

$$Q_p = \alpha \cdot Q_S + \beta \cdot Q_L = 0.5Q_S + 0.5Q_L \quad (3)$$

Where:

Q_S —Capacity estimation results based on SVM;

Q_L —Capacity estimation results based on LSTM;

α, β —Weighted values;

Q_p —Fused capacity estimation results.

Validate the fusion model with data of battery LIB3 and obtain the capacity estimation and error results shown in Figures 16 and 17. Mean Absolute Percentage Error (MAPE) and Root

Mean Square Error (RMSE) values are listed in Table 3.

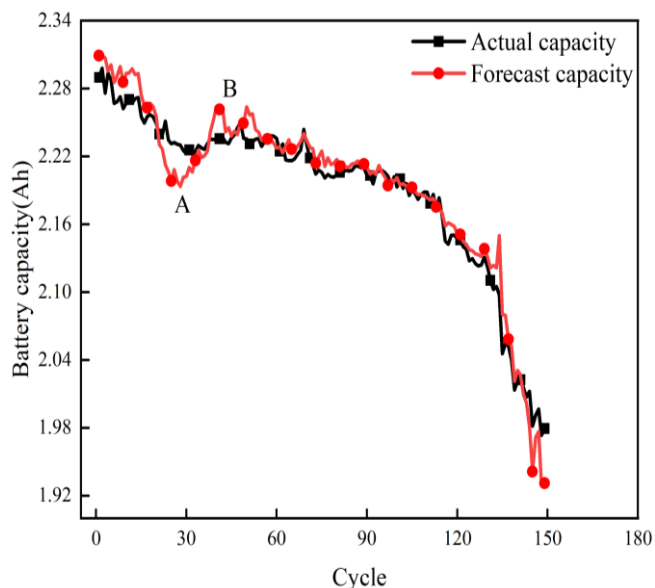


Figure 16. LIB3 Capacity estimation results based on SVM-LSTM fusion.

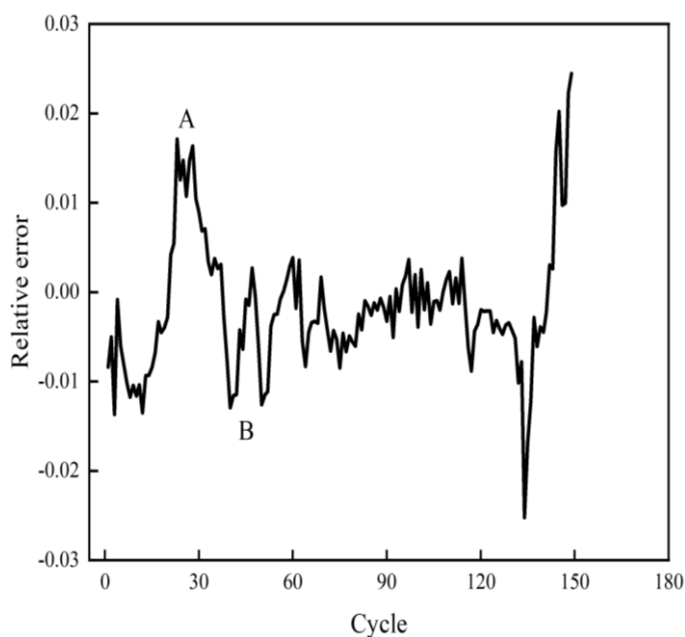


Figure 17. Relative errors of LIB3 capacity estimation based on SVM-LSTM fusion.

Table 3. Estimation errors of battery capacity.

| Network | Lithium-ion battery | Data set | MAPE / % | RMSE / Ah |
|----------|---------------------|-----------------|----------|-----------|
| SVM | LIB3 | Full life cycle | 1.13 | 0.034 |
| LSTM | LIB3 | Full life cycle | 1.45 | 0.0355 |
| SVM-LSTM | LIB3 | Full life cycle | 0.57 | 0.0163 |

(1) The predicted capacity of SVM-LSTM fusion model is highly consistent with the real capacity. There is no significant

abnormal point in the predicted value, and the relative error of the prediction is kept within 3% in the whole life cycle of battery. The results show that the use of SVM-LSTM fusion model can effectively reflect the relationship between the health features of lithium-ion battery and the degradation trend of available capacity. Such model also features both shallow neural network and deep learning network, thus embodying high precision and robustness.

(2) According to the estimation indexes of MAPE and RMAE, the SVM-LSTM fusion model offers significant higher precision and stability than either SVM or LSTM model. This further shows that the SVM-LSTM fusion model can realize a good combination of spatial observation and state update by better utilizing the spatial and temporal information of health features for lithium-ion battery. This process mode is similar with the idea of Kalman filter algorithm.

4.2. RUL prediction of lithium-ion battery

As the test object, battery LIB3 is regarded as a battery unit working in the real equipment, and its RUL is predicted when only the battery current and voltage data are available. In order to address this issue, this section includes three parts. First, estimate the historical available capacity of LIB3 in the working stage based on the trained SVM-LSTM fusion model. Then, train the LSTM model for predicting future capacity based on these estimated historical capacities. Finally, employ the trained LSTM network to predict the degradation trend of future capacity, and predict the RUL of battery LIB3 according to formula (4).

$$RUL = Cycle_{EOL} - Cycle_i \quad (4)$$

Where: $Cycle_{EOL}$ is the number of cycles by the end of life cycle for lithium-ion battery, which corresponds to the time when the battery's available capacity decayed to 80% of the rated capacity in this paper; $Cycle_i$ is the number of cycles at the forecast starting point.

We selected the first 50%, 60%, 70%, and 80% of historical capacity estimation data in the whole cycle periods as the training set, to forecast the available capacity of battery LIB3 in the remaining 50%, 40%, 30%, and 20% of the cycle periods. Figure 18 presents the trend of the predicted battery available capacity by the LSTM method for these four scenarios.

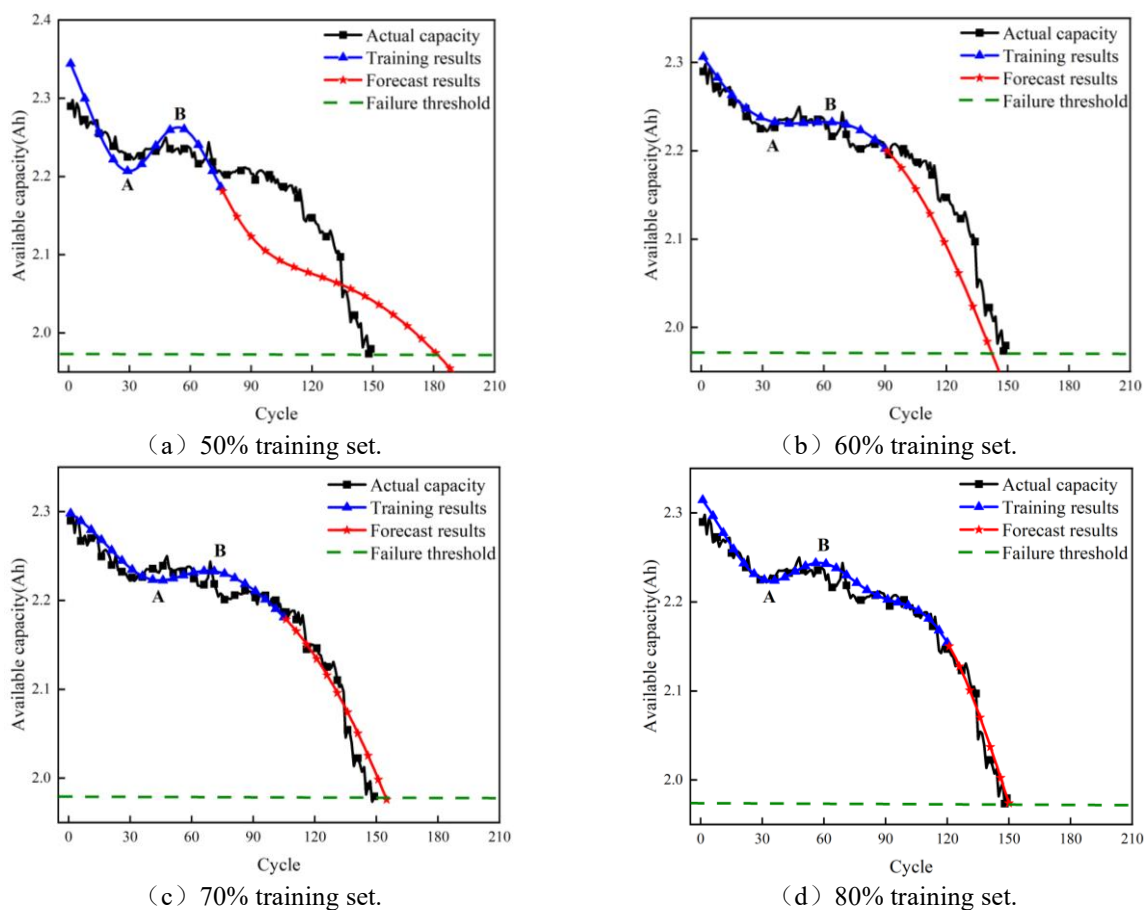


Figure 18. Forecast trends of available capacities for different forecast starting points.

It should be noted that, to simulate the situation when the battery's historical capacity data is unavailable in practices, the capacity data used here for model training is directly taken from LIB3 capacity estimation data in Figure 16. In the process of training based on the historical capacity estimation data, the precision of the RUL prediction model is greatly affected by the amount of training data. When 50% training data is adopted, the battery is in the early and middle stage of life cycle. Its capacity curve shows a changing trend of first decreasing and then increasing. The RUL prediction model focuses on the trend simulation of two inflection points A and B during training. As shown in Figure 16, the historical capacity estimation data shows relatively large errors at the inflection points A and B, which further increases the change gradient of battery capacity and strengthens the local fluctuation of the battery. The training error of RUL prediction model will inevitably increase in the process of training on this basis. With the gradual increase of battery training data, for RUL prediction model, the overall trend for the battery's life stage is emphasized, while the training precision of two local points A and B is ignored to some

extent, thus reducing the impact of battery capacity fluctuation on the RUL prediction model and effectively improving the overall precision of the RUL model in the whole training interval. The true values, predicted values and absolute error values of RUL for battery LIB3 at different starting points of prediction are listed in Table 4.

Table 4. RUL prediction results of LIB3 for different forecast starting points

| Forecast starting points | RUL true values | RUL predicted values | Absolute errors |
|--------------------------|-----------------|----------------------|-----------------|
| 50% | 74 | 104 | 30 |
| 60% | 59 | 51 | 8 |
| 70% | 44 | 50 | 6 |
| 80% | 29 | 30 | 1 |

In addition, the RUL prediction effects of battery LIB3 with Back Propagation (BP), Gate Recurrent Unit (GRU) and LSTM methods were compared. Figure 19 shows the absolute errors of the three prediction models at different prediction starting points.

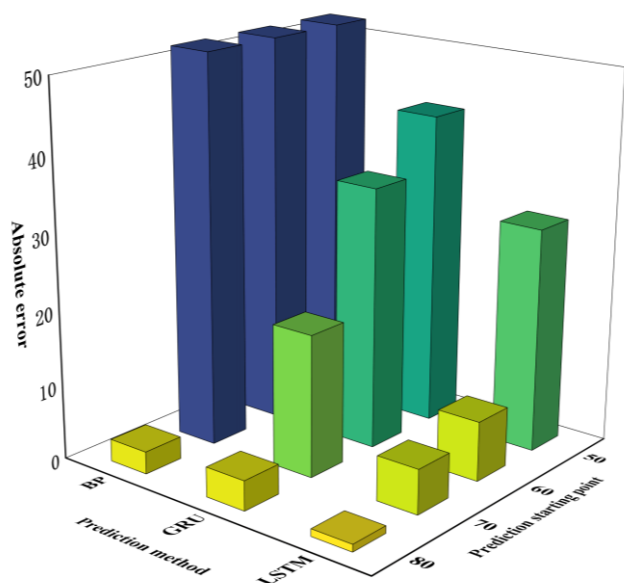


Figure 19. RUL prediction results of LIB3 with different methods.

It can be seen that when the starting point of prediction is gradually moved back, the amount of training data is gradually increased, the predicted RUL of lithium-ion battery is gradually close to the true RUL, and the absolute error of prediction is gradually reduced. When 80% of the battery data is used to train the RUL prediction model, the prediction precision is very high. The fluctuation degree of battery capacity degradation curve has great influence on RUL prediction. In order to simulate the regeneration phenomena of the battery in practice, a proper period of standing is deployed in the test, which leads to capacity recovery to a certain degree after standing, and violent fluctuation of the battery capacity degradation curve. In this case, small amount of data used for training will easily result in the dilemma of local fitting, thus leading to a large deviation between predicted RUL and real RUL. Therefore, the battery's capacity degradation curve for the complicated working conditions will inevitably show local fluctuation and strong nonlinearity. To ensure the precision of RUL prediction, enough training data input is required so that the use of training model can simulate the overall trend of battery degradation as much as possible.

Furthermore, as shown in Figure 19, the prediction accuracy of the LSTM network is superior to that of the GRU network and the BP network. Moreover, the LSTM network already demonstrates good prediction accuracy when the prediction starts at 60%. The LSTM network contains input gates, forget

gates, output gates, and memory cells. Compared to the GRU network and the BP network, the LSTM network has a more complex structure, which can better handle long-term dependencies and exhibits superiority in processing sequential data. Nevertheless, the GRU network only includes update gates and reset gates. Although it is faster during training and prediction, its effectiveness in handling tasks that require long-term dependency and memory is not as good as that of the LSTM network. When the prediction starting points are set as 50%, 60%, and 70%, the BP network cannot effectively capture the non-linear degradation trend of the battery, resulting in the predicted RUL exceeding the normal range. The phenomena is approximately depicted with the error results reaching the apex of the Z-axis. It further indicates that the BP network is constrained by its structure and performs poorly when making predictions in the early stages of degradation.

5. Conclusion

To address the difficulties of random charging and discharging and impossible battery capacity test in RUL prediction of lithium-ion battery under working conditions, this paper proposed a fusion model based RUL prediction method for battery. In terms of the complexity of charging and discharging behavior, based on the partial charging data, the feature space was constructed by synthesizing the traditional manual features and the features extracted by 1DCNN. A SVM-LSTM fusion model was explored to estimate the available capacity of lithium-ion battery, based on which, the LSTM model is applied to predict the RUL of lithium-ion battery. The research results indicate:

(1) The health features extracted by 1DCNN are highly correlated with the decay trend of battery capacity, showing high robustness. They can effectively make up for the restricted data deep mining in manual feature extraction. The constructed feature space includes features obtained both from machine learning and manual experience, which ensures the flexibility and completeness of feature extraction, and interpretability of feature extraction based on empirical knowledge. Such feature engineering is beneficial to improve the precision of capacity estimation and RUL prediction for lithium-ion battery.

(2) The established RUL prediction process can realize the real RUL prediction under the actual engineering background

when historical capacity data of battery is unknown. In order to accurately estimate the available capacity of battery, this paper proposes the SVM-LSTM fusion model, which fully explore the spatial and temporal relationship of features, realizing highly precise and stable estimation effect.

(3) When the LSTM method is applied for RUL prediction, the precision of prediction result is affected by the amount of historical capacity estimation precision and training data. As the starting point of prediction is moved backward and data in the training set is increased, the coincidence between the prediction trend of capacity degradation and the actual capacity change trend occurs increasingly, the absolute error of the predicted RUL of lithium-ion battery is gradually reduced, and the

prediction precision is greatly improved.

Although the proposed method can achieve high prediction accuracy, it has not focused on the problem of computational efficiency, which is another important consideration in practical applications. In addition, the paper only realizes the integration of two data-driven models, but the data-model interactive method that integrates battery mechanism model with data-driven model needs to be further explored to address complex working conditions, so as to obtain more accurate and robust prediction results. With the application of multiple sensors, it is also important to study the RUL prediction method based on multi-source data²².

Acknowledgments

The work is supported by the National Natural Science Foundation of China (72001192), the Natural Science Foundation of Henan Province (202300410490), the Key Scientific and Technological Program of Henan Province (232102240001). The authors also wish to thank them for their financial support.

References

1. Zheng Wenfang, Fu Chunliu, Zhang Jianhua, et al. Review of the remaining life prediction methods for lithium-ion battery. *Computer Measurement & Control* 28.12(2020):1-6.
2. Chen Wan, Cai Yanping, Su Yanzhao, et al. Research on indirect prediction method of remaining useful life of lithium-ion battery. *Chinese Journal of Power Sources* 45.06(2021):719-722+813.
3. Zhang, Yongzhi, et al. Long short-term memory recurrent neural network for remaining useful life prediction of lithium-ion batteries. *IEEE Transactions on Vehicular Technology* 67.7 (2018): 5695-5705. <https://doi.org/10.1109/TVT.2018.2805189>
4. Zheng Jili. Research on electrochemical behavior and optimization of lithium-ion batteries based on mechanism model. 2019. Harbin Institute of Technology, MA thesis.
5. Gambhire, Priya , et al. A physics based reduced order aging model for lithium-ion cells with phase change. *Journal of Power Sources* 270.dec.15(2014):281-291. <https://doi.org/10.1016/j.jpowsour.2014.07.127>
6. Waag, Wladislaw , et al. Application-specific parameterization of reduced order equivalent circuit battery models for improved accuracy at dynamic load. *Measurement* 46.10(2013):4085-4093. <https://doi.org/10.1016/j.measurement.2013.07.025>
7. Fotouhi, Abbas, et al. A review on electric vehicle battery modelling: From Lithium-ion toward Lithium–Sulphur. *Renewable and Sustainable Energy Reviews* 56 (2016): 1008-1021. <https://doi.org/10.1016/j.rser.2015.12.009>
8. Sun Daoming. Research on SOC and capacity estimation methods of power lithium-ion batteries. 2021. Zhejiang University, PhD dissertation.
9. Sun Dong, et al. State of Health Prediction of Second-Use Lithium-Ion Battery. *Transactions of China Electrotechnical Society* 33. 09 (2018): 2121-2129.
10. Li, Yi, et al. Data-driven health estimation and lifetime prediction of lithium-ion batteries: A review. *Renewable and sustainable energy reviews* 113 (2019): <https://doi.org/10.1016/j.rser.2019.109254>.
11. Tang, Xuliang, et al. Lithium-Ion Battery Remaining Useful Life Prediction Based on Hybrid Model. *Sustainability* 15.7 (2023): <https://doi.org/10.3390/su15076261>.
12. Liu, Yanshuo, et al. State-of-health estimation of lithium-ion batteries based on electrochemical impedance spectroscopy: a review. *Protection and Control of Modern Power Systems* 8.3 (2023): 1-17. <https://doi.org/10.1186/s41601-023-00314-w>
13. Long, Bing, et al. An improved autoregressive model by particle swarm optimization for prognostics of lithium-ion batteries.

Microelectronics Reliability 53.6 (2013): 821-831. <https://doi.org/10.1016/j.microrel.2013.01.006>

14. Wei, Jingwen, Guangzhong Dong, and Zonghai Chen. Remaining useful life prediction and state of health diagnosis for lithium-ion batteries using particle filter and support vector regression. *IEEE Transactions on Industrial Electronics* 65.7 (2018): 5634-5643. <https://doi.org/10.1109/TIE.2017.2782224>
15. Liu, Datong, et al. Lithium-ion battery remaining useful life estimation with an optimized relevance vector machine algorithm with incremental learning. *Measurement* 63 (2015): 143-151. <https://doi.org/10.1016/j.measurement.2014.11.031>
16. Hu, Yang, and Pengcheng Luob. Performance data prognostics based on relevance vector machine and particle filter. *Chemical Engineering* 33 (2013): 349-354.
17. Cao Mengda, et al. Remaining Useful Life Estimation for Lithium-ion Battery Using Deep Learning Method. *RADIO ENGINEERING* 51. 07 (2021): 641-648.
18. Wang Mingyan. Research on Remaining Useful Life Prediction Method of Lithium-ion Battery Based on Machine Learning.2023. Anhui University Of Science & Technology, MA thesis.
19. Li Chaoran, et al. An Approach to Lithium-Ion Battery SOH Estimation Based on Convolutional Neural Network. *Transactions of China Electrotechnical Society* 35.19(2020): 4106-4119.
20. GAO De-xin, LIU Xin, YANG Qing. Remaining Useful Life Prediction of Lithium-Ion Battery Based on CNN and BiLSTM Fusion. *INFORMATION AND CONTROL* 51. 03 (2022): 318-329+360.
21. Ma, Ning, et al. Prediction of the remaining useful life of supercapacitors at different temperatures based on improved long short-term memory. *Energies* 16.14 (2023): 5240. <https://doi.org/10.3390/en16145240>
22. Yi, Zhenxiao, et al. Sensing as the key to the safety and sustainability of new energy storage devices. *Protection and Control of Modern Power Systems* 8.1 (2023): 1-22. <https://doi.org/10.1186/s41601-023-00300-2>